Separation Science and Technology
Publication details, including instructions for authors and subscription information:
http://www.informaworld.com/smpp/title~content=t713708471

Fixed Bed Adsorptive Reactor for Ethyl Lactate Synthesis: Experiments, Modelling, and Simulation

Carla S. M. Pereira[a]; Viviana M. T. M. Silva[a]; Alírio E. Rodrigues[a]
[a] Laboratory of Separation and Reaction Engineering (LSRE), Associate Laboratory LSRE/LCM, Department of Chemical Engineering, Faculty of Engineering, University of Porto, Porto, Portugal

To cite this Article Pereira, Carla S. M. , Silva, Viviana M. T. M. and Rodrigues, Alírio E.(2009) 'Fixed Bed Adsorptive Reactor for Ethyl Lactate Synthesis: Experiments, Modelling, and Simulation', Separation Science and Technology, 44: 12, 2721 — 2749
To link to this Article: DOI: 10.1080/01496390903135865
URL: http://dx.doi.org/10.1080/01496390903135865

Separation Science and Technology, 44: 2721–2749, 2009

ISSN: 0149-6395 print/1520-5754 online
DOI: 10.1080/01496390903135865

Taylor & Francis
Taylor & Francis Group

Fixed Bed Adsorptive Reactor for Ethyl Lactate Synthesis: Experiments, Modelling, and Simulation

Carla S. M. Pereira, Viviana M. T. M. Silva, and Alírio E. Rodrigues
Laboratory of Separation and Reaction Engineering (LSRE), Associate Laboratory LSRE/LCM, Department of Chemical Engineering, Faculty of Engineering, University of Porto, Porto, Portugal

Abstract: Multicomponent adsorption equilibrium data were measured through binary adsorption experiments performed in a fixed bed column packed with Amberlyst 15-wet for the ethyl lactate system, at 20°C and 50°C. A novel approach based on the multicomponent Langmuir isotherm was used assuming a constant monolayer capacity in terms of volume for all species, reducing the adjustable parameters from 8 to 5, for each temperature. Reactive adsorption experiments were performed and used to validate a mathematical model developed for both fixed bed and simulated moving bed reactors, which involves velocity variations due to the change of multicomponent mixture properties.

Keywords: Adsorptions, amberlyst 15s, esterifications, green solvents, lactic acids, multifunctional reactors, simulated moving bed reactors

INTRODUCTION

Ethyl lactate is an important organic ester, considered biodegradable and produced by renewable resources, being used as a food additive, in perfumery, flavor chemicals, and solvent (1). It is a desirable coating for wood, polystyrene, and metals and also acts as a very effective paint

Received 28 December 2008; accepted 12 May 2009.
Address correspondence to Alírio E. Rodrigues, Laboratory of Separation and Reaction Engineering, Associate Laboratory LSRE/LCM, Department of Chemical Engineering, Faculty of Engineering, University of Porto, Rua Dr. Roberto Frias s/n, Porto 4200-465, Portugal. Tel.: 351 22 508 1671; Fax: 351 22 5081674. E-mail: arodrig@fe.up.pt

stripper and graffiti remover. Ethyl lactate has the capacity to dissolve a wide range of polyurethane resins, due to its high solvency power, being an excellent cleaner for the polyurethane industry. In the last years, a considerable growth in environmental regulation has been noticed (2) making ethyl lactate a very important product, since it is a green solvent and could replace a range of environment-damaging halogenated and toxic solvents as N-methyl Pyrrolidone (NMP), toluene, acetone, and xylene (3). Beyond all these applications, ethyl lactate can also be used in the pharmaceutical industry as a dissolving/dispersing excipient for various biologically active compounds without destroying the pharmacological activity of the active ingredient. It proved to be a very effective agent for solubilizing biologically active compounds that are difficult to solubilize in usual excipients (4).

The conventional way to produce ethyl lactate is by the esterification of lactic acid with ethanol in the presence of an acid catalyst, according to the reaction:

$$\text{Ethanol} + \text{LacticAcid} \overset{H^+}{\longleftrightarrow} \text{EthylLactate} + \text{Water}$$

The conversion of this kind of reaction is limited by chemical equilibrium; therefore, the technology for the industrial preparation of esters involves two consecutive steps. The first is the reaction itself, which stops when the equilibrium is reached. The second is the separation of the products from the equilibrium mixture containing products and unconverted reactants. The disadvantage of this technology is in its economics, because of the high energy costs and investment in several reaction and separation units. Multifunctional reactors, where reaction and separation take place into a single unit, allow, in addition to obvious savings in equipment costs, significant improvements in process performance for reactions limited by chemical equilibrium. By removing one of the products from the reaction zone, the equilibrium limitation can be overcome and the conversion can be driven to completion.

In the esterification reaction between lactic acid and ethanol the catalyst used is usually concentrated sulphuric acid (5). However, its application has several drawbacks (as separation problems and corrosion of equipment) and, thus, the use of heterogeneous catalysts is preferable. Among these types of catalysts, strongly acid resins, like Amberlyst 15-wet (A15), are of great interest in the case of reversible reactions, as esterifications and acetalizations, since they can act as catalyst and also as selective adsorbent (6–11). Accordingly, the synthesis of ethyl lactate in a chromatographic reactor using the A15 resin is very attractive. The simulated moving bed reactor (SMBR) is one of the most interesting chromatographic reactors and has been applied to several reversible

reactions catalyzed by acidic resins (7,8,12–17) improving the reaction conversion, given that the products are formed and simultaneously separated and removed from the reaction medium in two different streams (extract and raffinate). In order to provide a better understanding of the performance of the SMBR and to validate kinetic and adsorption data it is appropriate to evaluate first the dynamic behavior of the fixed bed adsorptive reactor (10,11,18–20). The present work addresses the detailed experimental study of the ethyl lactate synthesis in a fixed bed adsorptive reactor in order to validate the mathematical model to be later used to define the operating conditions of the SMBR. Binary adsorption experiments were carried out on a fixed bed packed with A15 resin, in the absence of reaction, at 293.15 and 323.15 K, to determine the multicomponent adsorption parameters. An SMBR experiment was performed to check the applicability of this technology for the production of ethyl lactate.

EXPERIMENTAL SECTION

Chemicals and Catalyst/Adsorbent

The chemicals used in the experiments were ethanol (>99.9% in water), lactic acid (>85% in water), and ethyl lactate (>98% in water) from Sigma-Aldrich (U.K.)

The column was packed with Amberlyst 15-wet (A15), which is a highly cross-linked polystyrene-divinylbenzene ion exchange resin functionalized with sulfonic groups (SO_3H), that acts as catalyst and adsorbent in this system. The properties of the A15 resin are presented in Table 1. A15 is a macroreticular-type resin, but according to Ihm et al. (21) only 4% of the active sites are located at the macropores (surface of the microspheres) and the others 96% are inside gel polymer microspheres.

These kinds of resins swell selectively in the presence of a liquid phase constituted of a multicomponent mixture. The swelling is due to the

Table 1. Physical and chemical properties of resin A15

Properties	A15
Manufacturer	Rohm and Haas
Concentration of acid sites (eq H^+/kg)	4.7
Surface area (m^2/g)	53
Average pore diameter (nm)	30
Particle diameter (mm)	0.3–1.2

sorption of the different components of the mixture, depending on their relative affinities to the resin. The polymeric resins that contain sulfonic acid functional groups, like the A15, exhibit a strong selectivity for polar species. Mazzotti and his co-workers (20) studied the sorption equilibrium of acetic acid, ethanol, water, and ethyl acetate on A15. They verified that the components can be listed by the following decreasing order of affinity to the resin: water, ethanol, acetic acid, and ethyl acetate and that the swelling ratio is 1.52, 1.48, 1.30, and 1.22 respectively. This conclusion agrees with the polarity of the components. So, it is expected for the system hereby presented that the order of the decreasing affinity of the components to the resin will be: water, ethanol, lactic acid, and ethyl lactate. The swelling effect might change the length and the bulk porosity of the fixed bed reactor; however, in the system under study, just a insignificant variation in the bed length was noticed and, therefore, a constant bed length was considered.

Experimental Apparatus

The experiments were performed in a laboratory-scale jacketed glass column that was maintained at constant temperature through a thermostatic bath (293.15 or 323.15 K), at atmospheric pressure (see Fig. 1). The experimental breakthrough curves were obtained by analyzing with a gas

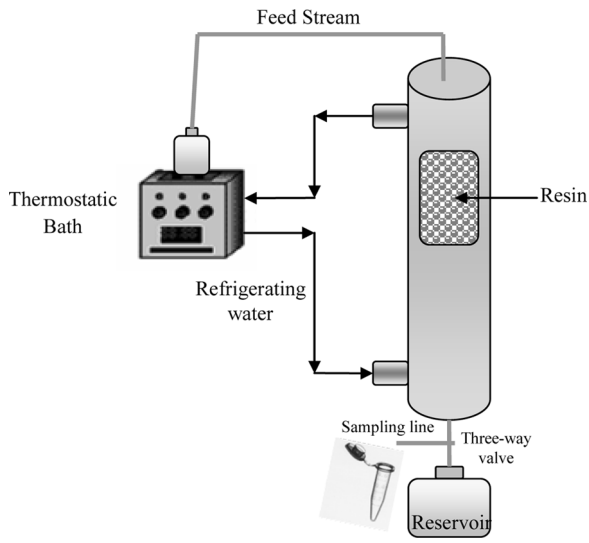

Figure 1. Experimental set-up (configuration: top-down flow direction).

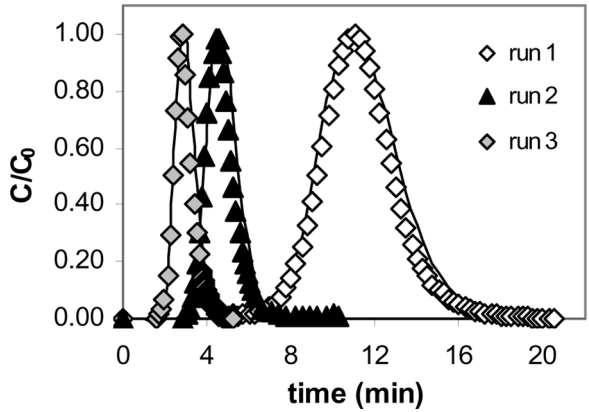

Figure 2. Tracer experiments using a blue dextran solution. Points are experimental values and lines are simulated curves.

chromatograph, small samples withdrawn at different times from the column exit.

Bed Porosity and Peclet Number

The bed porosity and the Peclet number were determined by pulse experiments of the tracer using a blue dextran solution ($5\,kg/m^3$), which is a polymer whose molecule is large enough (M.W. = 2,000,000) to diffuse only in the bulk fluid phase between resin particles. Samples of the blue dextran solution ($0.2\,cm^3$) were injected under different flow rates and the column response was monitored using a UV-VIS detector at 300 nm. The bed porosity was calculated from the stoichiometric time of the obtained experimental curves. An average Peclet number was obtained for the range of flow rates to be used in the fixed bed experiments by calculating the second moment of the experimental curves. Figure 2 shows the different tracer experiments performed and the respective values of bed porosity and Peclet number are presented in Table 2. The characteristics of the fixed bed column are summarized in Table 3.

Table 2. Results obtained from tracer experiments

	Q (mL/min)	τ (min)	ε	σ^2	Pe
run 1	1.985	11.23	0.347	3.528	71.48
run 2	4.981	4.69	0.364	0.556	79.24
run 3	8.026	2.92	0.365	0.229	74.54

Table 3. Characteristics of the fixed bed column

Solid weight (A15)	25 g
Length of the bed (L)	12 cm
Internal diameter (D_i)	2.6 cm
Average radius of resin beads (r_p)	372.5 μm
Bulk density (ρ_b)	390 Kg/m^3
Bed porosity (ε)	0.36
Resin particle porosity (ε_p)	0.36 [19]
Peclet number	75

Analytical Method

All the samples removed from the column exit were analyzed in a gas chromatograph (Chrompack 9100, Netherlands) using a fused silica capillary column (Chrompack CP-Wax 57 CB, 25 m x 0.53 mm ID, df = 2.0 μm) to separate the compounds and a thermal conductivity detector (TCD 903 A) to quantify it. The column temperature was programmed with a 1.5 min initial hold at 110°C, followed by a 50°C/min ramp up to 190°C and held for 8.5 min. The injector and detector temperature was maintained at 280°C and 300°C, respectively. Helium N50 was used as the carrier gas with a flowrate of 10.5 mL/min.

MODELLING OF FIXED BED

Several mathematical models have been developed to explain the kinetic behavior of the fixed adsorptive reactor and to predict the breakthrough curves. In order to interpret correctly the behavior of a fixed bed adsorptive reactor, it is necessary to characterize on one hand the partitioning equilibrium on the solid sorbent and on the other hand the reaction kinetics on the solid catalyst. A rigorous modelling of the sorption in the swelling polymer should include an appropriate model to predict the polymer-phase activities. Mazzoti and co-workers (8) used the extended Flory–Huggins model to determine the chemical activities of the species in the polymer phase for the esterification of acetic acid to ethyl acetate in the presence of A15 ion exchange resin catalyst. They assumed, in their kinetic model, that the activities of the species in the bulk liquid phase (estimated by UNIFAC method) were in equilibrium with the ones in the resin polymer phase (estimated by the extended Flory–Huggins model). However, in latter papers (19,22), it is mentioned that the extended Flory–Huggins model is not well suited for high cross-linked resins bearing highly polar groups on almost all monomers

and should be regarded as an empirical tool to correlate the equilibrium data and to predict the behavior of multicomponent mixtures. Yu (23) and collaborators state that using the extended Flory–Huggins model based on adsorption equilibrium data is not viable for most adsorption systems, given that nonreactive binary mixtures are scarce in the literature and the model involves complexity and inconvenience in computation. Thus, an alternative approach based on the multicomponent Langmuir model was considered in this work, since it is able to represent satisfactorily the experimental adsorption data and is simpler than the Flory-Huggins model. Nevertheless, it has to be mentioned that one of the assumptions of the Langmuir model considers that the monolayer adsorption has energetically equal binding sites, which do not describe the actual physical adsorption phenomena. Therefore, Pöpken and co-workers (22) proposed a multicomponent Langmuir adsorption isotherm which assumes a constant monolayer capacity in terms of mass for all species, after having measured mono-component adsorption data expressed in terms of volumes, masses, and moles of different species per gram of A15. In this work we will consider a constant volumetric monolayer capacity for all species, which will reduce the adjustable adsorption parameters from 8 (one molar monolayer capacity and one equilibrium constant for each component) to 5 (one volumetric monolayer capacity for all components and one equilibrium constant for each component).

A detailed model was used to describe the dynamic behavior of the fixed bed adsorptive reactor taken into account the following assumptions:

- Isothermal operation;
- The flow pattern is described by the axial dispersed plug flow model;
- External and internal mass transfer for absorbable species is combined in a global resistance;
- Constant column length and packing porosity;
- Extended Langmuir Isotherm model for multicomponent adsorption;
- Velocity variations due to changes in bulk composition.

The model equations are constituted by the following system of four second-order partial differential equations in the bulk concentration of the ith component (C_i), four ordinary differential equations in the average concentration of the ith component into the particle pores ($\overline{C}_{p,i}$), and four algebraic equations in the adsorbed concentration in equilibrium with $\overline{C}_{p,i}(\overline{q}_i)$:

Bulk fluid mass balance to component i:

$$\frac{\partial C_i}{\partial t} + \frac{\partial (uC_i)}{\partial z} + \frac{(1-\varepsilon)}{\varepsilon}\frac{3}{r_p}K_{L,i}\left(C_i - \bar{C}_{p,i}\right) = D_{ax}\frac{\partial}{\partial z}\left(C_T\frac{\partial x_i}{\partial z}\right) \qquad (1)$$

where $K_{L,i}$ is the global mass transfer coefficient of the component i, ε is the bed porosity, t is the time variable, z is the axial coordinate, D_{ax}, and u are the axial dispersion coefficient and the interstitial velocity respectively, r_p is the particle radius and x_i is the component molar fraction in liquid phase.

The axial dispersion coefficient D_{ax} was calculated from the Peclet number:

$$Pe = \frac{uL}{D_{ax}} \tag{2}$$

The interstitial fluid velocity variation is calculated using the total mass balance:

$$\frac{du}{dz} = -\frac{(1-\varepsilon)}{\varepsilon}\frac{3}{r_p}\sum_{i=1}^{NC} k_{L,i} V_{mol,i}\left(C_i - \overline{C}_{p,i}\right) \tag{3}$$

where $V_{mol,i}$ is the molar volume of component i.

Pellet mass balance to component i:

$$\frac{3}{r_p} K_{L,i}\left(C_i - \overline{C}_{p,i}\right) = \varepsilon_P \frac{\partial \overline{C}_{p,i}}{\partial t} + \left(1-\varepsilon_p\right)\frac{\partial \overline{q_i}}{\partial t} - \frac{v_i \rho_b}{1-\varepsilon} r\left(\overline{C}_{p,i}\right) \tag{4}$$

Where v_i is the stoichiometric coefficient of component i, ρ_b is the bulk density, ε_P is the particle porosity, $\overline{q_i}$ is the average adsorbed phase concentration of species i in equilibrium with $\overline{C}_{p,i}$, and $\boldsymbol{r}$ is the kinetic rate of the chemical reaction relative to the average particle concentrations in the fluid phase given by (24):

$$r = k_c \frac{a_{Eth} a_{La} - a_{EL} a_W / K_{eq}}{\left(1 + \sum_{i=1}^{NC} K_{s,i} a_i\right)^2} \tag{5}$$

where k_c is the kinetic constant, $K_{s,i}$ is the adsorption constant for species i and K_{eq} is the equilibrium reaction constant, a is the species activity (calculated by UNIQUAC model) and the subscripts *Eth, La, EL*, and W refer to ethanol, lactic acid, ethyl lactate and water, respectively. Kinetic and thermodynamic parameters, essential for Eq. (5), were taken from the literature (24) and are given in Table 4.

Table 4. Kinetic and thermodynamic parameters (24)

Temperature (K)	k_c(mol/(g.min))	$K_{s,w}$	$K_{s,Eth}$	K_{eq}
293.15	0.035	15.82	4.16	3.34
323.15	0.225	15.77	3.71	3.93

The Langmuir Adsorption equilibrium isotherm to component *i*:

$$\overline{q}_i = \frac{Q_i K_i \overline{C}_{p,i}}{1 + \sum_{j=1}^{NC} K_j \overline{C}_{p,j}} \tag{6}$$

where $Q_i = Q_V / V_{mol,i}$, Q_V is the volumetric monolayer capacity, $V_{mol,i}$ is the molar volume of specie *i*, and K_i is the equilibrium constant for component *i*.

Initial and Danckwerts boundary conditions:

$$t = 0 \qquad C_i = \overline{C}_{p,i} = C_{i,0} \tag{7}$$

$$z = 0 \qquad uC_i - D_{ax} C_T \left.\frac{\partial x_i}{\partial z}\right|_{z=0} = uC_{i,F} \tag{8}$$

$$z = L \qquad \left.\frac{\partial C_i}{\partial z}\right|_{z=L} = 0 \tag{9}$$

where subscripts *F* and 0 refer to the feed and initial states, respectively.

The proposed model considers a global mass transfer coefficient (K_L) defined, for each component, as:

$$\frac{1}{K_L} = \frac{1}{k_e} + \frac{1}{\varepsilon_p k_i} \tag{10}$$

wherein k_e and k_i are, respectively, the external and internal mass transfer coefficients to the liquid phase.

Santacesaria and co-workers (25) showed that the internal mass transfer coefficient varies in time, and the calculation of the rigorous values requires the solution of the complete model equations inside particles. As an approximation, the mean value estimated by Eq. (11) (26) was used:

$$k_i = \frac{5 D_m / \tau}{r_p} \tag{11}$$

The external mass transfer coefficient was estimated by the Wilson and Geankoplis correlation (27):

$$Sh_p = \frac{1.09}{\varepsilon} \left(Re_p\, Sc\right)^{0.33} \qquad 0.0015 < Re_p < 55 \tag{12}$$

where Sh_p and Re_p are, respectively, the Sherwood and Reynolds numbers, relative to particle:

$$Sh_p = \frac{k_e d_p}{D_m} \tag{13}$$

$$Re_p = \frac{\rho d_p u}{\eta} \tag{14}$$

and Sc is the Schmidt number:

$$Sc = \frac{\eta}{\rho D_m} \tag{15}$$

The infinite dilution diffusivities were estimated by the Scheibel correlation (28) which modified the Wilke-Chang equation in order to eliminate the association factor:

$$D^0_{A,B}(cm^2/s) = \frac{8.2 \times 10^{-8} T}{\eta_B Vmol_A^{1/3}} \left[1 + \left(\frac{3 Vmol_B}{Vmol_A}\right)^{2/3}\right] \tag{16}$$

where $D^0_{A,B}$ is the diffusion coefficient for a dilute solute A into a solvent B, T is the temperature, $V_{mol,i}$ is the molar volume of the component i, η_B is the viscosity of solvent B. Table 5 shows the diffusion coefficients for all binary systems:

For binary systems, Vignes equation (29) was used to predict $D_{A,B}$ in concentrated solutions from the infinite dilute coefficients as a simple function of composition:

$$D_{2,1} = D_{1,2} = \left(D^0_{1,2}\right)^{x_2} \left(D^0_{2,1}\right)^{x_1} \tag{17}$$

For concentrated multicomponent systems there are several mixing rules (30) to predict the molecular diffusivity coefficient of a solute in a mixture. In this work the Perkins and Geankoplis method was used (31):

$$D_{A,m}\eta_m^{0.8} = \sum_{\substack{i=1 \\ i \neq A}}^{n} x_i D^0_{Aj} \eta_i^{0.8} \tag{18}$$

where η_i is the viscosity of pure component i and η_m is the viscosity of the mixture. The viscosities of the mixtures play an important role in

Table 5. Diffusion coefficients for the binary mixtures estimated using the Scheibel correlation (Eq. (16))

$D^{\circ}_{i,j}$ (cm^2/s)	Ethanol	Lactic acid	Ethyl lactate	Water
Ethanol	0	1.6796E-06	2.583E-05	2.3655E-05
Lactic acid	2.5056E-05	0	2.1087E-05	2.0236E-05
Ethyl lactate	1.8034E-05	9.8526E-07	0	1.5444E-05
Water	8.2195E-05	4.6733E-06	7.4567E-05	0

the estimation of the diffusion coefficient. The methods used to predict binary and multicomponent mixtures viscosities are detailed in the Appendix.

In this model, the mixture viscosity and the components diffusivities in the liquid mixture were calculated at each time and at every axial position; therefore, the mass transfer parameters also depend on the liquid composition (estimated at each time and axial position from the equations presented).

Numerical Solution

The model equations were solved numerically using the gPROMS-general PROcess Modelling System version: 3.0.3 (www.psentreprise.com). gPROMS is a software package for modelling and simulation of processes with both discrete and continuous as well as lumped and distributed characteristics. The mathematical model involves a system of partial and algebraic equations (PDAEs). Third-order orthogonal collocation over twenty-one finite elements was used in the discretization of axial domain. The system of ordinary differential and algebraic equation (ODAEs) was integrated over time using the DASOLV integrator implementation in gPROMS. For all simulations a tolerance was fixed equal to 10^{-7}.

RESULTS AND DISCUSSION

Adsorption Isotherm

As the resin A15 acts simultaneously as adsorbent and as catalyst, in order to have information on the adsorptive equilibrium alone it is necessary to perform experiments with nonreactive binary mixtures. So, the breakthrough curves of ethanol, lactic acid, ethyl lactate, and water were measured in the absence of reaction. The resin was saturated with a certain component A and then the feed concentration of component B was changed stepwise. The experimental data were used to calculate the number of moles adsorbed/desorbed of each component for all the experiments. The adsorption parameters were optimized by minimizing the difference between experimental and theoretical values, according to Eq. 23:

$$n_{\text{exp}}^{ads} = Q \int_0^{\infty} [C_F - C_{out}(t)]dt \tag{19}$$

$$n_{\exp}^{des} = Q \int_0^{\infty} [C_{out}(t) - C_F]dt \tag{20}$$

$$n_{theo}^{ads} = \left(\left[\varepsilon + (1-\varepsilon)\varepsilon_p\right](C_F - C_0) + (1-\varepsilon)\left(1-\varepsilon_p\right)[q(C_F) - q(C_0)]\right)V \tag{21}$$

$$n_{theo}^{des} = \left(\left[\varepsilon + (1-\varepsilon)\varepsilon_p\right](C_0 - C_F) + (1-\varepsilon)\left(1-\varepsilon_p\right)[q(C_0) - q(C_F)]\right)V \tag{22}$$

$$fob = \sum_{k=1}^{NE} \left[\left(n_{\exp}^{ads} - n_{theo}^{ads}\right)^2 + \left(n_{\exp}^{des} - n_{theo}^{des}\right)^2\right] \tag{23}$$

Binary Adsorption Experiments

As mentioned above, for the determination of the adsorption parameters over the A15 resin it was necessary to perform experiments with nonreactive pairs of species. The possible binary mixtures to run the breakthrough experiments in the absence of the reaction are ethanol/water, ethyl lactate/ethanol and lactic acid/water. In all the experiments, the correct liquid flow direction (bottom-up or top-down) was considered in order to obtain reproducibility in the experimental results, since the hydrodynamic regime has an important effect on them and the difference in densities of the species can lead to axial backmixing driven by natural convection. The densities of ethanol, lactic acid, ethyl lactate, and water at 293.15 K are 0.79 g/cm^3, 1.21 g/cm^3, 1.04 g/cm^3, and 1 g/cm^3, respectively. The concentration fronts moving within the column are hydrodynamically stable if the component above the front is less dense than the component below the front (10). The multicomponent adsorption equilibrium was measured at two different temperatures, 293.15 K and 323.15 K. In Table 6 the optimized adsorption parameters and the molar volumes at the two temperatures are presented.

In order to compare the selectivity of the resin to the components, two different experiments were performed. One, where ethanol is fed to the column initially saturated with water, and the other, where ethanol is fed to the column initially saturated with ethyl lactate (see Fig. 3). In the first case (Fig. 3(a)) the concentration front of ethanol has a dispersive character and in the second one (Fig. 3(b)) the ethanol concentration front is self-sharpening. This is due to the fact that water is the preferentially adsorbed component and ethyl lactate is the weakest adsorbed component.

Table 6. Adsorption parameters over A15 resin

Component	Q_V (ml/$l_{wet\ solid}$) 20°C/50°C	Q(mol/$l_{wet\ solid}$) 20°C/50°C	K(l/mol) 20°C/50°C	V_{mol}(ml/mol) 20°C/50°C
Ethanol	390.0/383.5	6.70/6.30	5.443/3.068	58.17/60.87
Lactic acid		5.22/4.94	4.524/4.085	74.64/77.56
Ethyl lactate		3.42/3.23	1.117/1.815	113.99/118.44
Water		21.57/20.58	15.353/7.055	18.08/18.63

The experimental and theoretical concentration history for the binary mixture ethanol/water is shown in Fig. 4. Comparing the experimental amount of water adsorbed in the experiment of Fig. 4(a) with the experimental amount of water desorbed in the experiment of Fig. 4(b), the error obtained is 0.3%. For ethanol, the error between the amount adsorbed, Fig. 4(b), and the amount eluted, Fig. 4(a) is 0.31%. The deviations found between the experimental amount adsorbed of water and the one predicted by the model is of 4%, while in the case of ethanol the difference between the experimental amount adsorbed and predicted is of 0.6%.

The experimental and simulated results for the nonreactive binary mixture ethanol/ethyl lactate are shown in Fig. 5. The difference obtained between the experimental amount of ethyl lactate eluted in the experiment of Fig. 5(b), and the experimental amount of ethyl lactate adsorbed in the experiment of Fig. 5(a), was 0.21%. In the case of ethanol, the error obtained between the experimental amount adsorbed, Fig. 5(b), and the experimental amount eluted, Fig. 5(a), was 4.22%:

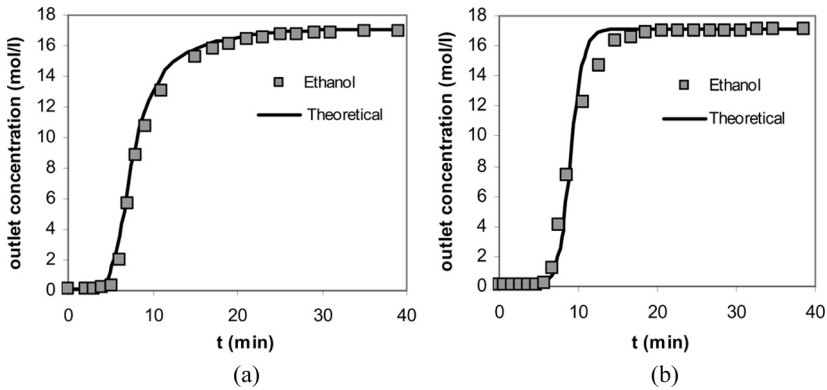

Figure 3. Breakthrough experiments: outlet concentration of ethanol as a function of time; Q = 5 mL/min; T = 293.15 K; top-down direction flow; (a) ethanol displacing water; (b) ethanol displacing ethyl lactate.

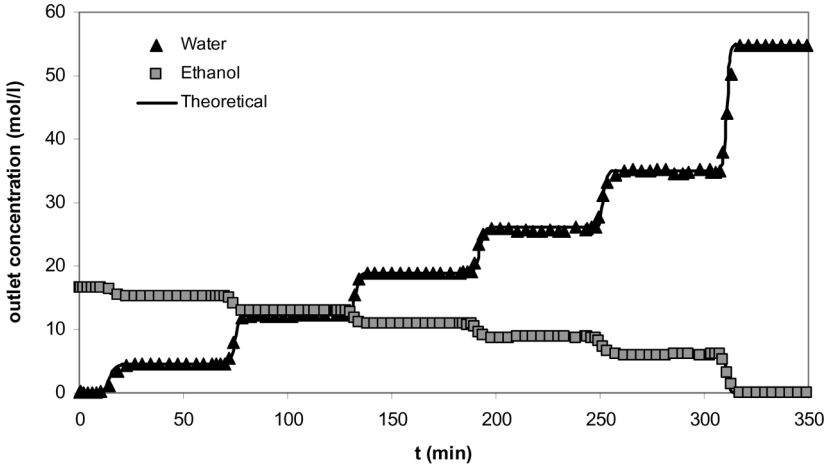

(a)

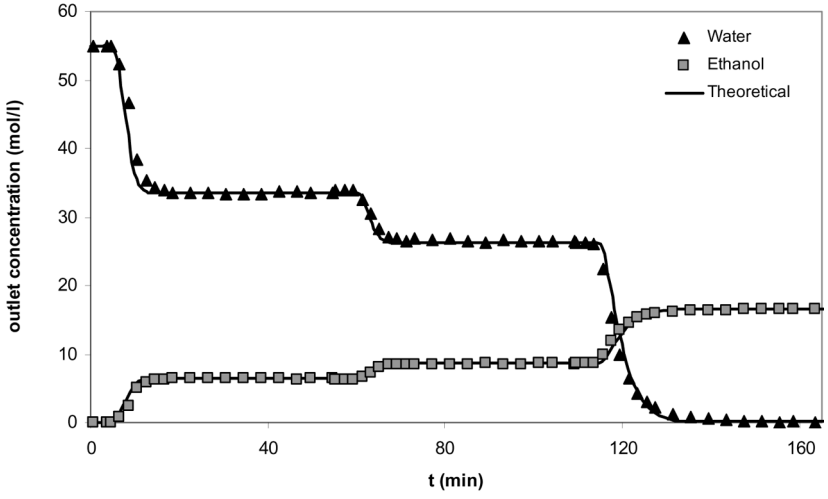

(b)

Figure 4. Breakthrough experiments: outlet concentration of ethanol and water as a function of time; $Q = 5\,mL/min$; $T = 323.15\,K$; (a) water displacing ethanol; Bottom up flow direction; (b) ethanol displacing water; Top-down flow direction.

For the nonreactive pair lactic acid/water (Fig. 6) the deviation found between the experimental amount of lactic acid eluted (Fig. 6(b)) and adsorbed (Fig. 6(a)) was 0.45% and between the experimental amount of water adsorbed (Fig. 6(b)) and eluted (Fig. 6(a)) was –1.07%.

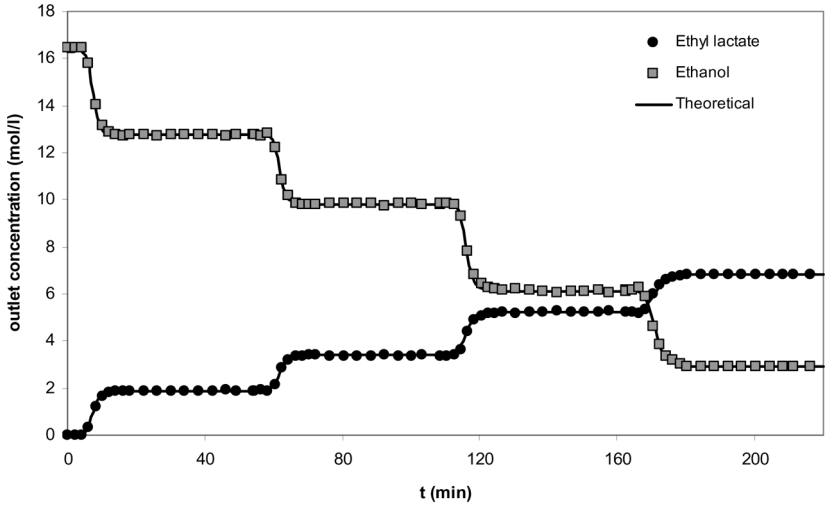

(a)

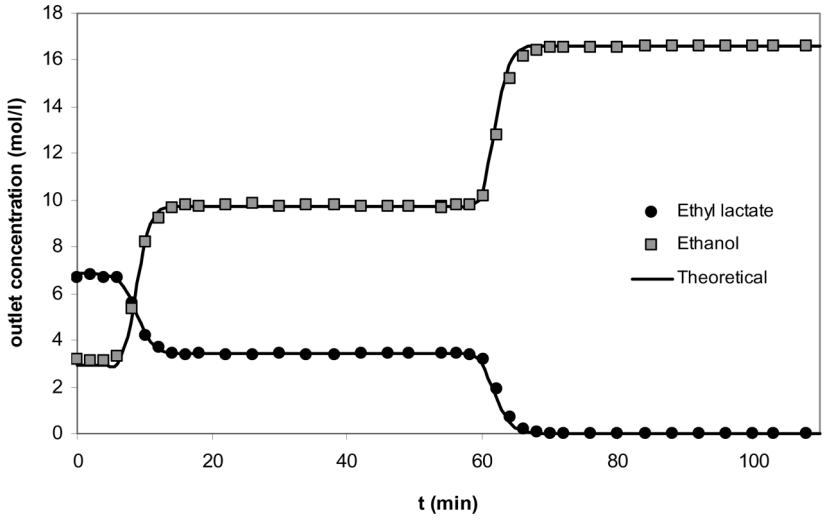

(b)

Figure 5. Breakthrough experiments: outlet concentration of ethanol and ethyl lactate as a function of time; $Q = 5\,mL/min$; $T = 323.15\,K$; (a) ethyl lactate displacing ethanol; Bottom up flow direction (b) ethanol displacing ethyl lactate; Top-down flow direction.

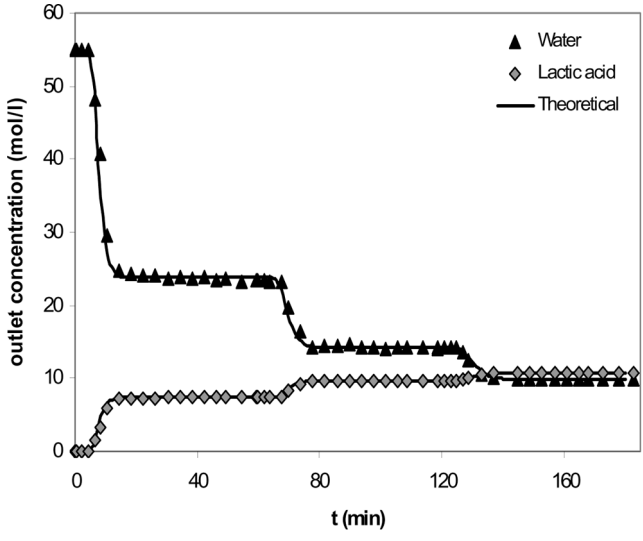

(a)

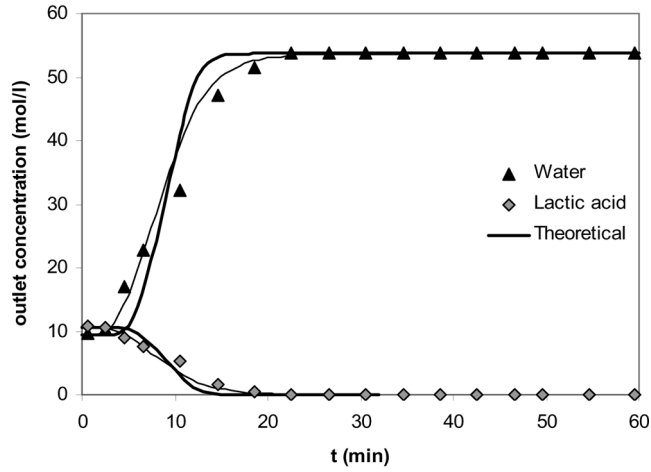

(b)

Figure 6. Breakthrough experiments: outlet concentration of water and lactic acid as a function of time; $Q = 5\,mL/min$; $T = 323.15\,K$; (a) lactic acid displacing water; Bottom up flow direction (b) water displacing lactic acid; Top–down flow direction.

All the binary adsorption experiments performed are very well described by the model, except for the case of the experiment of Fig. 6(b), where pure water displaces an 86 wt% lactic acid solution.

This could be explained by the water/lactic acid high selectivity in A15 (about 7.2); however, this behavior was not observed in the binary experiments ethanol/water where the selectivity is very similar (about 7.5).

Therefore, that behavior might be due to viscous fingering phenomenon, since the highest viscous fluid (85% lactic acid solution: 9.40 cP at 323.15 K), is being displaced by the lowest viscous fluid (water: 0.55 cP at 323.15 K), in the top-down direction, inducing an instable interface between them. The difference in their viscosities is of about 9 cP and in this case fingering effects are significant as mention by Catchpoole et al. (32). Viscous fingering is not accounted for in the global mass transfer coefficient (Eq. 10). In order to verify this assumption, the effect of viscous fingering can be described increasing the axial dispersion, as mentioned by Mallmann and co-authors (33). Indeed, the theoretical curve using an axial dispersion coefficient increased by a factor of 7 (thin line in Fig. 6(b)) fits the experimental data very well.

From the data reported it can be concluded that the most adsorbed component in A15 is water followed by ethanol and lactic acid, being the less adsorbed the ethyl lactate, as expected due to the polarity of the species.

Kinetic Experiments

Fixed Bed Reactor

A reaction experiment was performed in the chromatographic reactor packed with A15 initially saturated with ethanol, at 20°C. As shown in Fig. 7, the lactic acid conversion is very low due to both mass transfer and reaction kinetics limitations. Therefore, the fixed bed reactor was operated at 50°C in order to reduce mass transfer resistance and to increase reaction kinetics.

A mixture of ethanol and lactic acid was fed to the reactor saturated with ethanol and the concentration history of ethanol, lactic acid, ethyl lactate, and water at the end of the column is shown in Fig. 8(a).

As the lactic acid solution enters the column it is adsorbed and reacts with ethanol to produce ethyl lactate and water in the stoichiometric amount. Ethyl lactate is first eluted, since it has less affinity with the resin than water. This process continues until the equilibrium is reached; the resin is completely saturated with water and lactic acid. At this moment the selective separation of ethyl lactate and water is no longer possible. The local compositions remain constant and the steady state is achieved

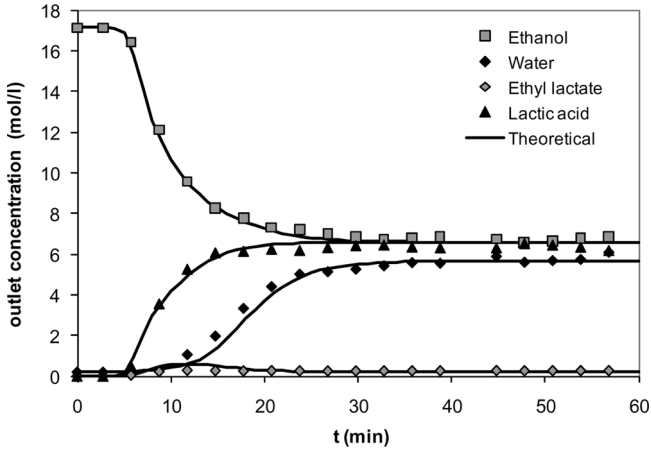

Figure 7. Concentration histories at the outlet of the fixed bed adsorptive reactor; column initially saturated with ethanol and then fed with a mixture of ethanol and lactic acid solution: $Q = 4.6\,\text{mL/min}$, $T = 293.15\,K$, $C_{La,F} = 6.76\,\text{mol/L}$, $C_{Eth,F} = 6.76\,\text{mol/L}$ and $C_{W,F} = 5.45\,\text{mol/L}$.

being the outlet stream constituted by a reactive mixture at the equilibrium composition. Analyzing the outlet concentration curves of ethyl lactate and water, shown in Fig. 8(a), a difference between them is noticed although they are formed at the same stoichiometric amount. This is related to the difference in the adsorbed amount of these species in the resin and, mainly, due to the fact that in the feed there is already some water content due to the lactic acid solution.

A second experiment was performed by only feeding the lactic acid solution (86 wt% in water) to the fixed bed adsorptive reactor (see Fig. 8(b)), in order to validate the model under very different conditions. Similarly to the previous experiment, as the lactic acid and water enter the column, they are adsorbed and start displacing the initially adsorbed ethanol. Simultaneously, the lactic acid reacts with ethanol in the resin phase until complete depletion of the adsorbed ethanol and the formed ethyl lactate is adsorbed, forming a dispersive front with ethanol once this is more adsorbed than ethyl lactate. The adsorption of the lactic acid solution continues till the resin saturation, displacing the ethyl lactate. Finally, lactic acid and water exit the column, water being the last eluted component due to high affinity of A15 towards this specie.

After the steady state is achieved and to perform a new reaction experiment it is necessary to first regenerate the column. This step

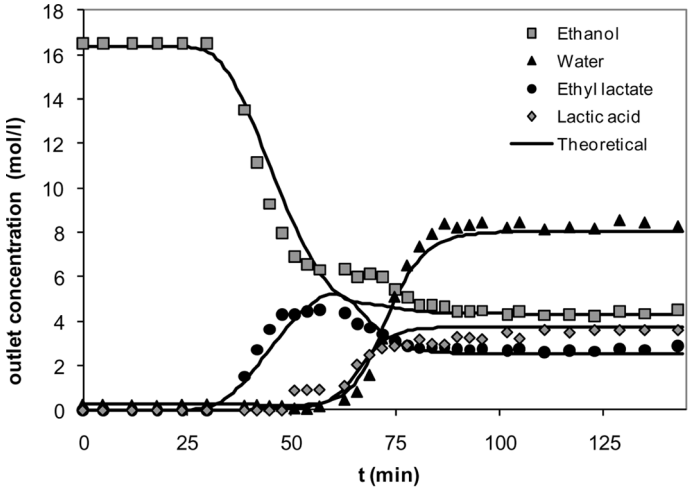

(a)

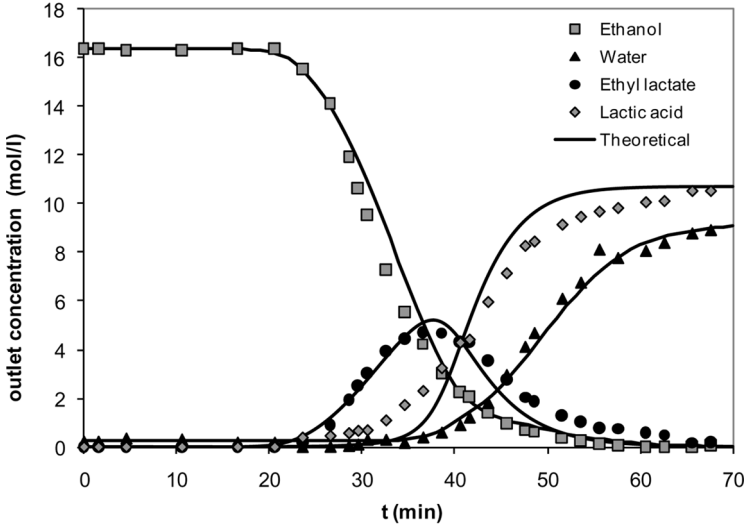

(b)

Figure 8. Concentration histories at the outlet of the fixed bed adsorptive reactor for production steps. (a) Experiment 1: Column initially saturated with ethanol and then fed with lactic acid solution (86 wt% in water). $Q = 1.3\,\text{mL/min}$, $T = 323.15\,\text{K}$. (b) Experiment 2: Column initially saturated with ethanol and then fed with a mixture of ethanol and lactic acid solution. $Q = 1.0\,\text{mL/min}$, $T = 323.15\,\text{K}$, $C_{La,F} = 5.88\,\text{mol/L}$, $C_{Eth,F} = 6.60\,\text{mol/L}$ and $C_{W,F} = 5.87\,\text{mol/L}$. b) Regeneration Step: Column fed with ethanol. $Q = 4.4\,\text{mL/min}$; $T = 323.15\,\text{K}$.

requires the use of a solvent to displace the adsorbed species. The solvent used was ethanol, since a lactic acid solution could not be used, because it contains water and then the column would not be completely regenerated. In Fig. 9, the regeneration steps for each experiment are presented.

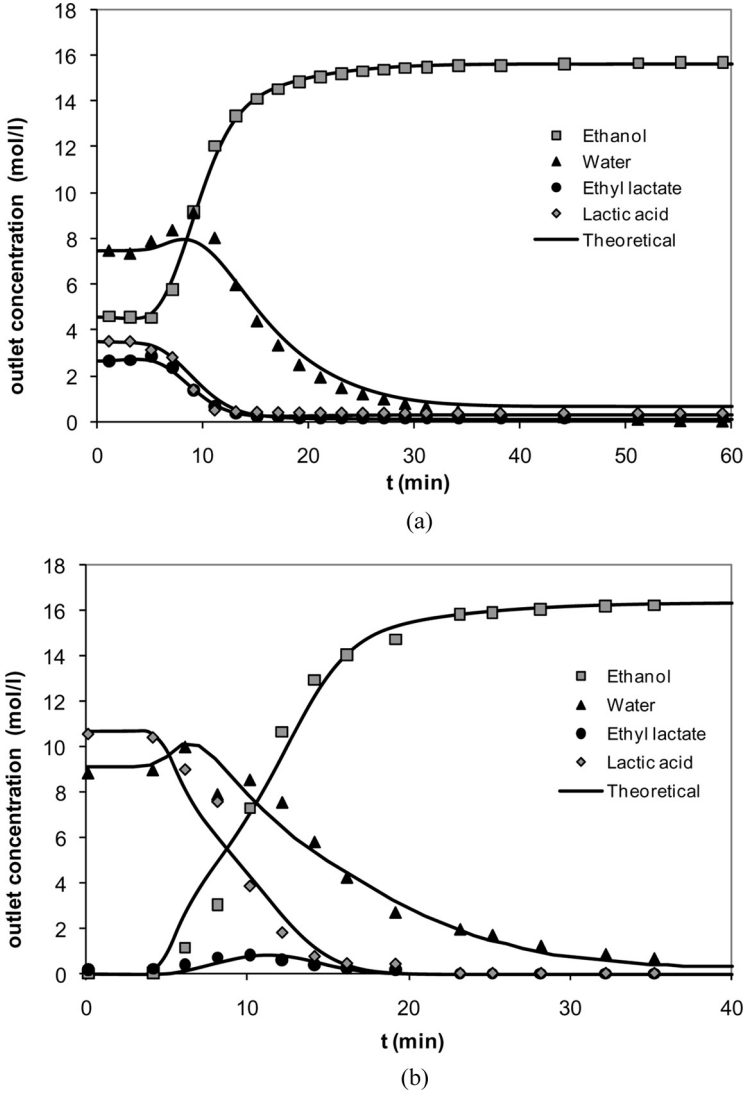

Figure 9. Concentration histories at the outlet of the fixed bed adsorptive reactor for regeneration steps with ethanol ($Q = 4.3\,\text{mL/min}$, $T = 323.15\,\text{K}$). (a) Experiment 1. (b) Experiment 2.

As expected, ethyl lactate and lactic acid are rapidly desorbed; however, a large amount of ethanol is required in order to completely desorb all water.

All the experimental results obtained for both production and regeneration steps, at 293.15 and 323.15 K, are well described by the proposed mathematical model.

Simulated Moving Bed Reactor

The synthesis of ethyl lactate was performed at 323.15 K in a SMBR pilot unit LICOSEP 12–26 (Novasep, France) with twelve columns packed with the acid resin A15 and configuration 3–3-4-2. The feed was lactic acid (86 wt% in water) and the desorbent was ethanol. The flowrates of feed, raffinate, and extract streams were $Q_F = 1.8\,\text{mL/min}$, $Q_R = 8.8\,\text{mL/min}$, $Q_X = 20.4\,\text{mL/min}$, respectively, and the time switch was of 2.9 min. The experimental concentration profiles are presented in Fig. 10.

In the experiment of Fig. 10, 100% conversion of lactic acid was obtained; but the purities obtained were just 74% of ethyl lactate in the raffinate port and 95% of water in the extract port. However, changing some operating parameters, as the switching time and the flowrates, higher ethyl lactate purity can be obtained. In order to find the optimized

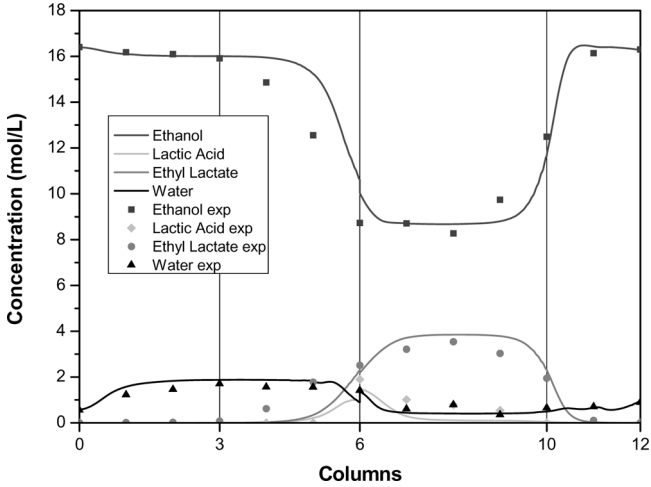

Figure 10. Experimental concentration profiles in a SMBR at the middle of the switching time at cyclic steady-state (13th cycle). Conditions: $Q_F = 1.8\,\text{mL/min}$, $Q_R = 8.8\,\text{mL/min}$, $Q_X = 20.4\,\text{mL/min}$, $t^* = 2.9\,\text{min}$, $T = 323.15\,\text{K}$.

operating parameters and to achieve the best SMBR performance an extensive study is in progress.

CONCLUSIONS

A detailed study of the ethyl lactate synthesis in a fixed bed adsorptive reactor was carried out. Adsorption experiments in the absence of reaction at 20°C and 50°C were performed. For each temperature, the adsorption parameters were obtained: single volumetric monolayer capacity for all components and one equilibrium constant for each component. A mathematical model for the fixed bed adsorptive reactor was developed which includes: axial dispersion, external and internal mass transfer resistances, multicomponent Langmuir adsorption isotherm, the reaction rate measured in a previous work, and velocity variations due to mixture of molar-volume variations. This model proved to be efficient in the prediction of the reaction and regeneration steps performed in the fixed bed reactor and it will be very useful for the study of the SMBR for the synthesis of ethyl lactate.

One experiment was performed at a pilot scale SMBR LICOSEP 12–26 unit with twelve columns packed with the A15 resin. The performance parameters obtained were lactic acid conversion of 100% and raffinate and extract purities of 74% and 95%, respectively. These results pointed out that the SMBR is a very interesting technology for the ethyl lactate production.

ACKNOWLEDGEMENTS

Carla S.M. Pereira gratefully acknowledges to *Fundação para a Ciência e a Tecnologia* (FCT, Portugal) the PhD Research Fellowships SFRH/BD/23724/2005. This work was also supported by the project POCI/EQU/61580/2004 (FCT, Portugal).

NOTATION

a	liquid phase activity
C	liquid phase concentration (mol/m^3)
C_r	total liquid phase concentration (mol/m^3)
$\overline{C_p}$	average liquid phase concentration inside the particle (mol/m^3)

df	film thickness (μm)
d_p	particle diameter (m)
$D^0_{A,B}$	diffusion coefficient for a dilute solute A into a solvent B (m^2/s)
$D_{A,B}$	mutual diffusion coefficient for binary concentrated solutions (m^2/s)
D_{ax}	axial dispersion (m^2/s)
D_m	molecular diffusivity (m^2/s)
$G_{1,2}$	interaction parameter in Eq. (A.1)
K	Langmuir equilibrium parameter (m^3/mol)
k_i	internal mass transfer coefficient (m/s)
k_e	external mass transfer coefficient (m/s)
k_c	kinetic constant ($mol/kg_{res} \cdot s$)
K_{eq}	equilibrium constant
K_s	adsorption constant in Eq. (5).
K_L	global mass transfer coefficient (m/s)
L	bed length (m)
n	number of moles (mol)
Pe	Peclet number
$\overline{q}$	average solid phase concentration in equilibrium with $\overline{C_p}$ (mol/m^3_{res})
Q	molar adsorption capacity, defined as $Q_i = Q_v/V_{mol,i}$ (mol/m^3_{res})
Q_F	volumetric flowrate of the feed, m^3/min
Q_V	volumetric monolayer capacity (m^3/m^3_{res})
Q_R	volumetric flowrate of the raffinate (m^3/min)
Q_x	volumetric flowrate of the extract (m^3/min)
Q_D	volumetric flowrate of the desorbent (m^3/min)
r	reaction rate relative to fluid concentration inside the particle ($mol/kg_{res} \cdot s$)
r_p	particle radius (m)
Re_p	Reynolds number relative to particle
Sh_p	Sherwood number relative to particle
Sc	Schmidt number
T	temperature (K)
t	time (s)
t^*	switching time (min)
u	interstitial velocity (m/s)
V_{mol}	molar volume in the liquid phase (m^3/mol)
V	volume of the bulk (m^3)
x	liquid phase molar fraction
z	axial coordinate (m)

Greek Letters

ε	bulk porosity
ε_p	porosity of pellet
η	fluid viscosity ($kg/m \cdot s$)
η_m	mixture viscosity ($kg/m \cdot s$)
ϕ	volume fraction
ν	stoichiometric coefficient
ρ	liquid density (kg/m^3)
ρ_h	bulk density (kg_{res}/m^3)
τ	tortuosity

Subscripts

o	relative to initial conditions
exp	experimental
F	relative to the feed
i	relative to component *i* (i = Eth, La, EL, W)
out	at the end of the fixed bed column
p	relative to particle
theor	theoretical
Eth	relative to ethanol
La	relative to Lactic acid
EL	relative to ethyl lactate
W	relative to water
R	relative to raffinate
X	relative to extract

Superscripts

ads	adsorbed
des	desorbed

REFERENCES

1. Tanaka, K.; Yoshikawa, R.; Ying, C.; Kita, H.; Okamoto, K.-I. (2002) Application of zeolite T membrane to vapor-permeation-aided esterification of lactic acid with ethanol. *Chem. Eng. Sci.*, *57* (9): 1577–1584.
2. Cann, M.C. (2001) *Greening Across the Chemistry Curriculum, Including Web Based Teaching Modules. Green Chemistry in Education, NSF sponsored workshop*, Eugene, Oregon.
3. Datta, R.; Tsai, S.-P. (1998) Esterification of Fermentation-Derived Acids via Pervaporation. WO Patent 9823579, 1998.
4. Muse, J.; Colvin, H.A. (2005) Use of ethyl lactate as an excipient for pharmaceutical compositions. Patent 20050287179 A1.
5. Zhang, Y.; Ma, L.; Yang, J. (2004) Kinetics of esterification of lactic acid with ethanol catalyzed by cation-exchange resins. *React. Funct. Polym.*, *61* (1): 101–114.

6. Funk, G.A.; Lansbarkis, J.R.; Chandhok, A.K. (1995) Process for concurrent esterification and separation using a simulated moving bed. Patent 5,405,992.
7. Kawase, M.; Suzuki, T.B.; Inoue, K.; Yoshimoto, K.; Hashimoto, K. (1996) Increased esterification conversion by application of the simulated moving-bed reactor. *Chem. Eng. Sci.*, *51* (11): 2971–2976.
8. Mazzotti, M.; Kruglov, A.; Neri, B.; Gelosa, D.; Morbidelli, M. (1996) A continuous chromatographic reactor: SMBR. *Chem. Eng. Sci.*, *51* (10): 1827–1836.
9. Ruggieri, R.; Ranghino, G.; Carvoli, G.; Tricella, A.; Gelosa, D.; Morbidelli, M. (2003) Process for esterification in a chromatographic reactor. Patent 6,586,609.
10. Silva, V.M.T.M.; Rodrigues, A.E. (2002) Dynamics of a fixed-bed adsorptive reactor for synthesis of diethylacetal. *AIChE J.*, *48* (3): 625–634.
11. Gandi, G.K.; Silva, V.M.T.M.; Rodrigues, A.E. (2006) Synthesis of 1,1-dimethoxyethane in a fixed bed adsorptive reactor. *Ind. Eng. Chem. Res.*, *45* (6): 2032–2039.
12. Lode, F.; Francesconi, G.; Mazzotti, M.; Morbidelli, M. (2003) Synthesis of methylacetate in a simulated moving-bed reactor: Experiments and modeling. *AIChE J.*, *49* (6): 1516–1524.
13. Yu, W.; Hidajat, K.; Ray, A.K. (2003) Modeling, simulation, and experimental study of a simulated moving bed reactor for the synthesis of methyl acetate Ester. *Ind Eng Chem Res.*, *42* (26): 6743–6754.
14. Silva, V.M.T.M.; Rodrigues, A.E. (2005) Novel process for diethylacetal synthesis. *AIChE J.*, *51* (10): 2752–2768.
15. Pereira, C.S.M.; Gomes, P.S.; Gandi, G.K.; Silva, V.M.T.M.; Rodrigues, A.E. (2008) Multifunctional reactor for the synthesis of dimethylacetal. *Ind Eng Chem Res.*, *47* (10): 3515–3524.
16. Minceva, M.; Gomes, P.S.; Meshko, V.; Rodrigues, A.E. (2008) Simulated moving bed reactor for isomerization and separation of p-xylene. *Chem. Eng. J.*, *140* (1–3): 305–323.
17. Borges da Silva, E.A.; Ulson de Souza, A.A.; de Souza, S.G.U.; Rodrigues, A.E. (2006) Analysis of the high-fructose syrup production using reactive SMB technology. *Chem. Eng. J.*, *118* (3): 167–181.
18. Kawase, M.; Inoue, Y.; Araki, T.; Hashimoto, K. (1999) The simulated moving-bed reactor for production of bisphenol A. *Catal Today.*, *48* (1–4): 199–209.
19. Lode, F.; Houmard, M.; Migliorini, C.; Mazzotti, M.; Morbidelli, M. (2001) Continuous reactive chromatography. *Chem. Eng. Sci.*, *56* (2): 269–291.
20. Mazzotti, M.; Neri, B.; Gelosa, D.; Morbidelli, M. (1997) Dynamics of a chromatographic reactor: Esterification catalyzed by acidic resins. *Ind. Eng. Chem. Res.*, *36* (8): 3163–3172.
21. Ihm, S.K.; Chung, M.J.; Park, K.Y. (1988) Activity difference between the internal and external sulfonic groups of macroreticular ion-exchange resin catalysts in isobutylene hydration. *Ind. Eng. Chem. Res.*, *27* (1): 41–45.

22. Pöpken, T.; Götze, L.; Gmehling, J. (2000) Reaction kinetics and chemical equilibrium of homogeneously and heterogeneously catalyzed acetic acid esterification with methanol and methyl acetate hydrolysis. *Ind Eng Chem Res.*, *39* (7): 2601–2611.
23. Yu, W.; Hidajat, K.; Ray, A.K. (2004) Determination of adsorption and kinetic parameters for methyl acetate esterification and hydrolysis reaction catalyzed by Amberlyst 15. *Appl Catal A: Gen.*, *260* (2): 191–205.
24. Pereira, C.S.M.; Pinho, S.P.; Silva, V.M.T.M.; Rodrigues, A.E. (2008) Thermodynamic equilibrium and reaction kinetics for the esterification of lactic acid with Ethanol Catalyzed by acid ion exchange resin. *Ind Eng Chem Res.*, *47*: 1453–1463.
25. Santacesaria, E.; Morbidelli, M.; Servida, A.; Storti, G.; Carra, S. (1982) Separation of xylenes on Y zeolites. 2. Breakthrough curves and their interpretation. *Ind. Eng. Chem. Process. Des. Dev.*, *21* (3): 446–451.
26. Glueckauf, E. (1955) Theory of chromatography. *Trans. Faraday Soc.*, *51*: 1540–1551.
27. Ruthven, D.M. (1984) *Principles of Adsorption and Adsorption Processes*; Wiley & Sons: New York.
28. Scheibel, E.G. (1954) Correspondence. Liquid Diffusivities. Viscosity of Gases. *Ind. Eng. Chem.*, *46* (9): 2007–2008.
29. Vignes, A. (1966) Diffusion in binary solutions: Variation of diffusion coefficient with composition. *Ind. Eng. Chem. Fundam.*, *5* (2): 189–199.
30. Umesi, N.O.; Danner, R.P. (1981) Predicting diffusion coefficients in nonpolar solvents. *Ind. Eng. Chem. Proc. DD.*, *20* (4): 662–665.
31. Perkins, L.R.; Geankoplis, C.J. (1969) Molecular diffusion in a ternary liquid system with the diffusing component dilute. *Chem. Eng. Sci.*, *24* (7): 1035–1042.
32. Catchpoole, H.J.; Andrew Shalliker, R.; Dennis, G.R.; Guiochon, G. (2006) Visualising the onset of viscous fingering in chromatography columns. *J. Chrom. A.*, *1117* (2): 137–145.
33. Mallmann, T.; Burris, B.D.; Ma, Z.; Wang, N.H.L. (1998) Standing wave design of nonlinear SMB systems for fructose purification. *AlChE J.*, *44* (12): 2628–2646.
34. Grunberg, L.; Nissan, A.H. (1949) Mixture law for viscosity. *Nature.*, *164* (4175): 799–800.
35. Troupe, R.A.; Aspy, W.L.; Schrodt, P.R. (1951) Viscosity and density of aqueous lactic acid solutions. *Ind. Eng. Chem.*, *43* (5): 1143–1146.
36. Macias-Salinas, R.; Garcia-Sanchez, F.; Eliosa-Jimenez, G. (2003) An equation-of-state-based viscosity model for non-ideal liquid mixtures. *Fluid Phase. Equilib.*, *210* (2): 319–334.
37. Li, J.; Carr, P.W. (1997) Accuracy of empirical correlations for estimating diffusion coefficients in aqueous organic mixtures. *Anal. Chem.*, *69* (13): 2530–2536.
38. Gonzalez, B.; Calvar, N.; Gomez, E.; Dominguez, A. (2007) Density, dynamic viscosity, and derived properties of binary mixtures of methanol or ethanol with water, ethyl acetate, and methyl acetate at T = (293.15, 298.15, and 303.15) K. *J. Chem. Thermodyn.*, *39* (12): 1578–1588.

39. Motin, M.A.; Kabir, M.H.; Huque, M.E. (2005) Viscosities and excess viscosities of methanol, ethanol and n-propanol in pure water and in water + surf excel solutions at different temperatures. *Phys. Chem. Liq.*, *43* (2): 123–137.

APPENDIX

One of the most used and recommended liquid mixture viscosity correlation is the one by Grunberg–Nissan (34), which for binary mixtures is:

$$\ln(\eta_m) = x_1 \ln(\eta_1) + x_2 \ln(\eta_2) + x_1 x_2 G_{1,2} \qquad \text{(A.1)}$$

where x_1 is the mole fraction of component i and $G_{1,2}$ is an empirical interaction parameter adjusted by experimental data.

For aqueous lactic acid solutions, the interaction parameters were found to be $G_{LA,W}(20^\circ C) = 5.240$ and $G_{LA,W}(50^\circ C) = 4.369$ using viscosities determined experimentally by Troupe and co-authors (35). As can be seen in Fig. A.1, the Eq. (A.1) describes well the viscosity in a large range, from diluted solutions till concentrated lactic acid (85% mass fraction).

For the system water ethanol, experimental data at 20°C (38) and 50°C (39) are not well fitted by Eq. A.1 ($G_{Eth,W}(20^\circ C) = 2.568$ and $G_{Eth,W}(50^\circ C) = 1.799$), as it can be seen in Fig. A.2. It was stated by

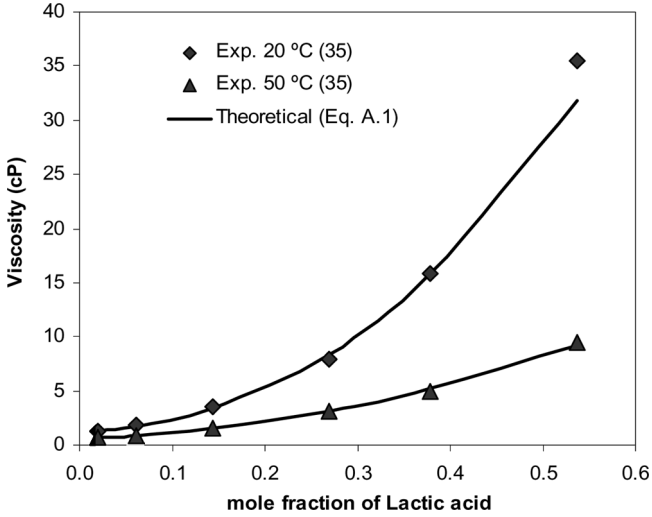

Figure A.1. Viscosities of aqueous lactic acid solutions.

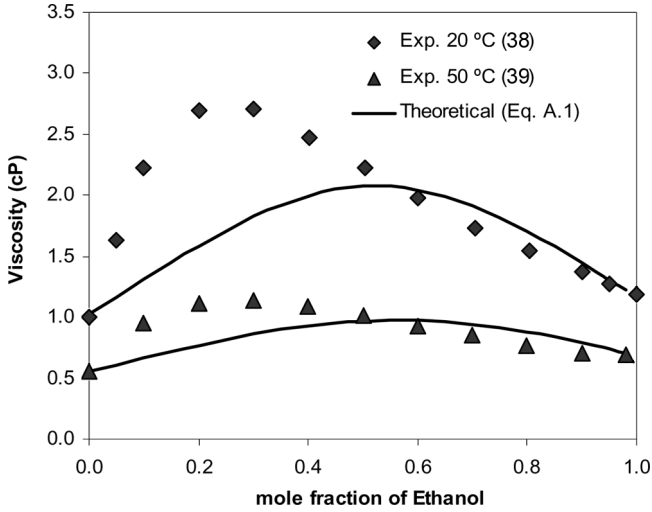

Figure A.2. Viscosities of ethanol/water mixtures. Solid line calculated by Eq. (A.1).

several authors, that the Grunberg–Nissan correlation is not suitable for several aqueous system (36,37). Normally, the correlation used to describe the viscosity of those systems involves at least 3 adjustable

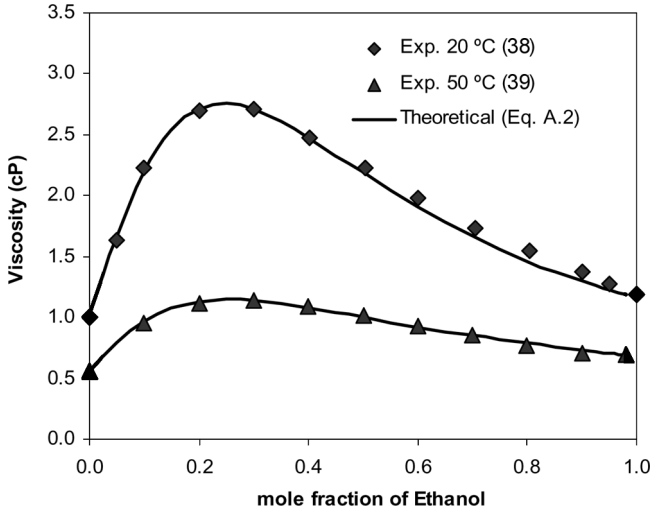

Figure A.3. Viscosities of ethanol/water mixtures. Solid line calculated by Eq. (A.2).

Table A.1. Viscosities of ethanol, lactic acid, ethyl lactate and water at 20°C and 50°C

Temperature	Ethanol	Lactic acid	Ethyl lactate	Water
20°C	1.1617	53.6564	2.5986	1.0254
50°C	0.6885	13.9919	1.1233	0.5530

parameters (38,39). We propose a new correlation with just one adjustable parameter similar to that of Grunberg–Nissan, but the excess viscosity function is averaged by the volume fractions instead of molar ones:

$$\ln(\eta_m) = x_1 \ln(\eta_1) + x_2 \ln(\eta_2) + \phi_1 \phi_2 G_{1,2} \tag{A.2}$$

Where x_i is the mole fraction of component i, ϕ_i is the volume fraction of component i and $G_{1,2}$ is an empirical interaction parameter adjusted by experimental data. Using the new interaction parameters in Eq. (A.2) ($G_{Eth,W}(20°C) = 3.833$ and $G_{Eth,W}(50°C) = 2.698$), the ethanol/water system viscosities are very well predicted, as it can be seen in Fig. A.3.

Since there are no experimental data available for the systems ethanol/ethyl lactate and ethanol/lactic acid, these systems are considered as ideal, i.e., $G_{Eth,EL} = 0$ and $G_{Eth,LA} = 0$.

The liquid viscosity of the multicomponent system ethanol, lactic acid, ethyl lactate and water is calculated by the following model:

$$\ln(\eta_m) = x_{Eth} \ln(\eta_{Eth}) + x_{LA} \ln(\eta_{LA}) + x_{EL} \ln(\eta_{EL}) + x_W \ln(\eta_W) + x_{LA} x_W G_{LA,W} + \phi_{Eth} \phi_W G_{Eth,W}. \tag{A.3}$$

The viscosities of pure components at 20 and 50°C are presented in Table A.1.